ELSEVIER

Atmospheric Research 61 (2002) 169–187

ATMOSPHERIC RESEARCH

www.elsevier.com/locate/atmos

Role of sulfate aerosols in modifying the cloud albedo: a closure experiment

S. Menon [a], V.K. Saxena [b,*], P. Durkee [c], B.N. Wenny [b], K. Nielsen [c]

[a] *NASA GISS/Columbia University, New York, NY, USA*
[b] *Department of Marine, Earth and Atmospheric Sciences, North Carolina State University, Raleigh, NC 27695-8208, USA*
[c] *Department of Meteorology, Naval Postgraduate School, Monterey, CA, USA*

Received 12 March 2001; received in revised form 20 August 2001; accepted 24 October 2001

Abstract

At a remote mountain-top location in the southeastern US, measurements were made to estimate the contribution of anthropogenic aerosols to the cloud albedo. The influence of the long-range transport of anthropogenic emissions on cloud microphysical and optical properties at the mountain top site was investigated. The sources of the cloud forming air masses were determined from back-trajectory analysis. Cloud water sulfate content was used as a surrogate for anthropogenic pollution. The effects of particulate sulfate on cloud condensation nuclei (CCN) concentration, cloud droplet number concentration (N), cloud droplet effective radii (R_{eff}) and cloud albedo were analyzed. A non-linear relationship between CCN and sulfate mass was obtained with a lowered sensitivity of CCN at high values of sulfate. Differences in N and sulfate from polluted to less polluted type air masses were much larger than that in R_{eff}. This could be due to the variability in cloud liquid water content (LWC) as R_{eff} is more related to LWC and cloud thickness than is N. The variability in cloud liquid water path (LWP) results in the optical depth being more sensitive to changes in R_{eff} than to N for differences in cloud pollutant content. As part of a "closure experiment", the cloud albedo calculated from in situ measurements for a 3-year period (1993–1995) compared well with that inferred from the Advanced Very High Resolution Radiometer (AVHRR) data. This accomplishes the objective of our closure experiment and proves that albedo of non-precipitating, thin, isolated clouds can be resolved against the dark forested background by AVHRR. The cloud reflectivity inferred from satellite measurements and that calculated from in situ observations were found to vary with the cloud water sulfate and N. Non-linear increases in satellite inferred cloud albedo with LWP

* Corresponding author. Tel.: +1-919-515-7290; fax: +1-919-515-7802.
E-mail address: saxena@eos.ncsu.edu (V.K. Saxena).

PII: S0169-8095(01)00140-5

suggest the importance of determining the contribution of cloud dynamic feedbacks on the indirect effect.

Keywords: Sulfate aerosols; Cloud microphysics; Cloud reflectivity; Satellite retrievals; Closure experiment

1. Introduction

Anthropogenic sulfate aerosols are known to affect climate by modifying the radiative properties for both clear and cloudy skies. The backscattering of short-wave radiation by anthropogenic sulfate aerosols in cloud-free air is referred to as the direct radiative forcing by sulfate aerosols. Because of their chemical nature and size distributions, sulfate particles are known to be efficient cloud condensation nuclei (CCN). Through its effect on the activation spectrum of CCN and the consequent effect on cloud microphysics and cloud optical thickness (τ), anthropogenic sulfates modify the short-wave albedo (Twomey, 1977; Schwartz and Slingo, 1996) of clouds and thereby, regional and global climate. This indirect radiative forcing by anthropogenic sulfate has been thought (Charlson et al., 1987, 1991; Boers et al., 1994) to be equal (though of opposite sign) to that caused by the doubling of anthropogenic CO_2. Carbonaceous and other non-sulfate aerosols are also important contributors to global climate change (Novakov and Penner, 1993; Rivera-Carpio et al., 1996; Hegg et al., 1997; Novakov et al., 1997). However, there is still no enough data on the properties and distribution of these aerosols on a global scale (see, for example, Kondratyev, 1999) to fully consider their climatic impact without much uncertainty.

Since aerosols have non-uniform sources and a short lifetime (of the order of a few days), the climatic effects of aerosols can be more easily deciphered on a regional scale. Dettinger et al. (1995) analyzed surface-air temperatures in the US for 1910–1987 and found a cooling trend for the southeastern region and long-term warming for the Southwest. This supports the findings of Saxena et al. (1997) who indicated a decrease of -0.28 °C in the average annual mean maximum temperature at 52 stations in the southeastern US during the period 1949–1994. A maximum in the negative forcing due to aerosols has been indicated for the southeastern US by modeling studies (Boucher and Lohmann, 1995; Jones et al., 1994). Thus, the forcing due to aerosols may be important for regional climate.

Measurements related to the changes in cloud microphysical properties due to the aerosol content of different air masses have been carried out in the past at locations such as the northeastern US (Leaitch et al., 1992, 1996), and Atlantic Ocean (Brenguier et al., 2000; Borys et al., 1998; Novakov et al., 1994; Garrett and Hobbs, 1995; Hudson and Li, 1995) to name a few. However, none has been carried out in the southeastern US over a land location. Due to theoretical limitations in modeling the aerosol effect on cloud microphysical properties, models rely on empirical relationships between aerosol mass and droplet number (Jones et al., 1994; Boucher and Lohmann, 1995; Menon et al., 2001) to predict the cloud radiative properties, though some models have now developed more deterministic approaches (e.g., Chuang et al., 1997; Lohmann et al., 1999; Ghan et al.,

2001). However, the issue of correctly determining cloud droplet number using either the prognostic or the diagnostic approach is still debatable. The impact of aerosols on regional climate suggests that many such regional measurements would be needed to fully comprehend the effects of aerosols on a global scale. Since most modeling studies indicate large negative forcings in the southeastern US, observations from that area are important for understanding the effect of aerosols on clouds and climate.

In this paper, we present the results of a *closure experiment* conducted at a regionally representative mountain-top location in the southeastern US during the summers of 1993–1995. The experiment consisted of intensive surface and available satellite observations. In a closure experiment, the measured value of a dependent parameter (such as cloud albedo) is *computed from observations of independent parameters* and the results are compared with *direct observations* of this dependent parameter. In our experiment, cloud albedo was inferred from the direct observations of AVHRR (Advanced Very High Resolution Radiometer) aboard the NOAA (National Oceanographic and Atmospheric Administration) satellites. The isolated, thin, non-precipitating clouds at the mountain-top were identified against the dark forested background. Surface observations in these clouds consisted of: CCN activation spectrum in the cloud forming air, cloud droplet number concentration (N) as a function of droplet radius, cloud liquid water content (LWC), and the cloud water chemistry. Effective cloud droplet radii (R_{eff}), cloud optical depth (τ), and cloud albedo were computed from these observations. Assuming sulfate in the cloud water as a surrogate for anthropogenic pollution, we present below an analysis of the effect of anthropogenic pollution on the cloud microphysical and optical properties.

2. Methodology

2.1. Field study description

The experimental site is located on Mount Gibbes in the Mount Mitchell State Park (2038 m msl, at 35°44′ 05″ N and 82°17′ 15″ W), NC, in the southeastern US. The site is ideal for in situ cloud measurements as nearly 7 out of 10 days have a cloud episode during the summer months (Saxena et al., 1989). A 17.1-m walk-up tower equipped with temperature, pressure, wind speed, wind direction and humidity instruments provide continuous measurements. A rotatable carriage, located on the tower's northern face, carries an Atmospheric Science Research Center passive string cloud water collector (ASRC) described by Kadlecek et al. (1983). Cloud droplet size distribution was obtained by means of a Particle Measuring System Forward Scattering Spectrometer Probe (FSSP) (Knollenberg, 1981) located below the cloud water collector. A cloud was designated and measurements commenced when visibility was reduced to 1 km for a continuous 15-min period. The type of clouds formed for cloud events that are less than 8 h in duration are usually those due to orographic lifting. Cloud events that last for more than 8 h usually have clouds that are influenced by frontal passages (Saxena and Lin, 1990).

The cloud thickness was obtained from representative soundings at the Mt. Mitchell site from the Hybrid Single Particle Lagrangian Integrated Trajectory (HY-SPLIT) model (Draxler, 1987) and was calculated as described in Saxena et al. (1996). The cloud top

is identified as that point on the sounding where the difference between ambient and dew point temperature is less than 5 °C. The surface pressure at the Mt. Mitchell site and the cloud top pressure are then converted to a physical thickness using the hypsometric equation, thus giving the vertical extent of the cloud above the Mt. Mitchell site. Sampling by cloud radar would probably lead to a better estimate of determining the cloud top and the thickness of the cloud layer. In the absence of such measurements, the cloud thickness determined from soundings, though subjective, serve as the best possible estimate.

The sources of the cloud forming air masses were analyzed from their back trajectories obtained from the HY-SPLIT model. The continental US is divided into three sectors: (1) the polluted continental (PC) sector located between 290° and 65° azimuth relative to Mt. Mitchell that is influenced by highly polluted air from the Ohio valley region; (2) the continental (C) sector between 210° and 290° that is influenced by relatively clean continental air from the great plains; and (3) the marine (M) sector between 65° and 210° that is influenced by clean maritime air from the ocean (Ulman and Saxena, 1997). This classification is based on the SO_x and NO_x emission inventory from the US Environmental Protection Agency (EPA, 1993). However, the marine air masses must traverse over some land before reaching the site, and hence is a modified marine air mass. The accuracy of the back trajectories, like all computed trajectories, is limited (Draxler and Stunder, 1988) and depends on a variety of factors including wind field resolution, the type of computational scheme used and the associated synoptic-scale meteorological conditions. Ulman and Saxena (1997) provide more details on the classification of the air masses and the trajectory analysis associated with the events for a previous data set that was from the Mt. Mitchell site.

2.2. Instrumentation

The cloud droplet number concentration was obtained from the FSSP cloud drop size distribution and R_{eff} was calculated as the ratio of the third and second moments of the droplet size distribution. The alignment of the optical measurement sensor is checked after every cloud event by recording the spectra that result when glass beads of varying sizes are introduced and is calibrated if the alignment is not proper. This is done by adjusting the resulting measured size to account for the difference in the index of refraction between glass and water (Baumgardner, 1983). The FSSP was factory calibrated at the beginning and end of each field season. The data are obtained every 5 s and are then averaged to obtain hourly averages that correlate to the hourly averages for the chemical and cloud water data. Details on the calibration procedure are in DeFelice and Saxena (1994) and calibration errors and measurement uncertainties are in Baumgardner (1983). For concentrations of less than 500 cm^{-3}, Baumgardner (1983) has estimated a 17% error for concentration and size measurements.

The cloud water collector was manually operated and cloud water samples were collected on an hourly basis upon the occurrence of a cloud event. The collector was cleaned by spraying distilled, deionized water on the collection strands before and after every cloud event, to remove traces of chemicals that may have been present from previous sampling. At the end of every cloud event, the collector was enclosed in a clean bag to avoid con-

tamination by dry aerosol impaction on the collection surfaces. The collected cloud water was used to calculate LWC in terms of mass per unit volume. The error possibility for the LWC estimated is about 34%. At high wind speeds (>12 m s^{-1}) all the droplets will not be collected as the droplets may fly off or get suspended in the upper or lower portions of the strings as was observed by DeFelice and Saxena (1990). For low wind speeds, the droplets that are collected usually range between 2 and 20 μm in diameter. For all cases reported in this paper, the wind speeds were low enough (between 2 and 12 m s^{-1}) to collect most of the measured spectra. However, it can be expected that at lower wind speeds all the measured spectra would not be collected. Details on the impaction efficiency, wind speed and droplet sizes for the ASRC collector are in McLaren et al. (1985) and in Menon et al. (2000).

The pH of the cloud water was immediately measured after collection and the cloud water sample was subsequently prepared and refrigerated for later ionic analysis via ion chromatography. The pH of a standard buffer solution was also measured at the same time as a check to ensure that the measured pH was accurate within ± 0.02 units. The concentration of eight ionic species namely SO_4^{2-}, NO_3^-, NH_4^+, Ca^{2+}, K^+, Mg^{2+}, Na^+ and Cl^- were analyzed from each cloud water sample by means of ion chromatography (Cl^-, SO_4^{2-}), flow injection analysis (NO_3^-, NH_4^+) and induced coupled plasma atomic emission spectroscopy (Ca^{2+}, K^+, Mg^{2+}, Na^+). Since we are mainly focussing on sulfates, we report the errors in sulfate concentrations alone. Also, previous results have shown a strong correlation between pH and cloud water sulfate concentrations for the 1993–1995 data sets indicating that the major contributor to cloud water acidity are sulfates and that sulfates are the dominant species in cloud water samples (Menon and Saxena, 1998). The errors in the other ionic concentrations are discussed in Menon et al. (2000). The instrument detection limit for SO_4^{2-} is 0.5 μmol l^{-1} and the method detection limit (MDL) is 2.5 μmol l^{-1}. Errors in reported concentrations are usually 10–15% for concentrations between 1 and 20 times the MDL values, between 5% and 10% for 20–200 times the MDL values and for values greater than 200 times the MDL values, errors are 2–5%. The percentage difference between measured values of the cations and anions from the cloud water samples were found to be less than 6% on average, indicating good ionic balance. The values that were beyond this error limit have not been reported and could represent errors in analyzing all the cations and anions or in determining the species concentrations.

Sulfate mass concentrations in μg m^{-3} were calculated by multiplying the cloud water sulfate content with the corresponding LWC. To avoid assumptions on scavenging efficiencies, we assume that the entire sulfate content in the air mass is scavenged in the cloud water in order to investigate the optimum effect of sulfates on cloud properties. Previous studies (e.g. Leaitch et al., 1986; Hegg and Hobbs, 1983) have suggested that $\sim 60-80\%$ of sulfate aerosols are scavenged in cloud water.

The CCN-Spectrometer (Fukuta and Saxena, 1979a,b) was operated from a shed located about 8 m to the north east of the tower. Its air intake is an inverted funnel (0.1 m diameter) that extends 0.5 m out from and whose opening is 2 m above the top of the shed as well as the canopy. The opening of this funnel is oriented perpendicular to the airflow past it. A particle analyzer with a built-in calibration check performs the CCN counting. The spectrometer provides a continuous measurement of the CCN number concentration as a function of supersaturations as described by DeFelice and Saxena (1994). The CCN

concentrations are calculated as $CCN = cS^k$, where c and k are determined from the distributions and S is the supersaturation. The maximum error in the CCN concentrations are given by $\Delta CCN = CCN\ (k(\Delta S\ S^{-1}))$, where ΔS is the difference between the measured quantity and its most likely value and is based on the error for using the linear vapor density profile in the CCN spectrometer plus the error due to reading off the position of the sampling inlet (Fukuta and Saxena, 1979a).

3. CCN-sulfate analysis

In order to illustrate the differences in cloud microphysical properties for polluted versus less polluted clouds, average values of sulfate, N, R_{eff} and LWC for M, PC and C type air masses, from simultaneous measurements obtained during the 1993–1995 field season, are listed in Table 1. Only non-precipitating cases were considered for all the analyses. Air masses that were purely marine were not sampled during the 1995 observational period (differences in N, R_{eff} and sulfate for M, C and PC cases from previous years are discussed in more detail in Menon and Saxena, 1998). In general, higher sulfate content, are observed for PC type air masses as compared to the C or M type air masses. However, an exception is the 1994 data set where higher sulfate values were obtained for the M air masses as compared to the C air masses although higher N values are observed for the C cases. The higher standard deviation for the sulfate for the C air masses suggests more variability in the sulfate content. Average values of sulfate, N and R_{eff} for the 3 years combined indicates over a factor of 3 increase in sulfate, a 92% increase in N and a decrease of 27% in R_{eff} as one moves from the marine to the polluted air mass. The PC type air masses had higher values of N and smaller R_{eff} as compared to the C or M type air masses with high LWC standard deviations indicating a high variability in the FSSP measurements. Differences in R_{eff} between PC, C or M air masses are not as high probably due to the variations in LWC since R_{eff} is more closely related to variations in LWC and cloud thickness. Therefore, CCN and N are usually more suitable indicators of differences in pollution in air masses.

The relationship between aerosol mass, CCN and N is an important link between aerosol and cloud properties and is dependent on factors such as regional location, supersaturation values, updraft speed and the presence of chemical species other than sulfates. In order to predict the indirect radiative effect of anthropogenic sulfates, most climate models (e.g., Rotstayn, 1999; Boucher and Lohmann, 1995; Lohmann and Feichter, 1997) make use of the empirical relationships between sulfate content and N/CCN. The N so obtained is then used to calculate the optical depth and cloud albedo from which changes in the radiative forcing are estimated for different sulfate contents.

Here, we present an investigation of the CCN-sulfate mass relationship for cases that had coincident CCN and sulfate measurements. Since CCN concentrations are only available for the 1995 field season, out of the 32 cases for the 1995 data reported in Table 1, we restrict our discussion to 14 cases that had coincident measurements. CCN concentrations are reported at 1% supersaturation to facilitate comparison with other measurements (e.g., Hegg, 1994). Usually, one would expect lower supersaturations (between 0.3% and 0.7%), which would imply reduced CCN concentrations. The CCN-

Table 1
Average values of cloud water sulfate content, cloud droplet number concentration (N), the effective radii (R_{eff}) of cloud droplets and cloud liquid water content (LWC) for air masses that arrived from either the marine (M), polluted continental (PC) or continental (C) sectors for the 1993–1995 field season

Years		Marine (M)				Continental (C)				Polluted Continental (PC)			
		SO_4^{2-} (μmol l^{-1})	N (cm^{-3})	R_{eff} (μm)	LWC (g m^{-3})	SO_4^{2-} (μmol l^{-1})	N (cm^{-3})	R_{eff} (μm)	LWC (g m^{-3})	SO_4^{2-} (μmol l^{-1})	N (cm^{-3})	R_{eff} (μm)	LWC (g m^{-3})
1993	Ave.	61	333	4.5	0.28	274	523	3.90	0.21	511	594	3.03	0.22
	SD	13	16	0.06	0.02	201	258	1.2	0.07	238	282	1.0	0.07
	No.	4	4	4	4	36	36	36	36	27	27	27	27
1994	Ave.	167	238	4.92	0.10	92	541	4.11	0.21	298	754	3.15	0.26
	SD	101	128	1.1	0.05	88	302	1.7	0.22	169	433	0.74	0.51
	No.	16	16	16	16	42	42	42	42	14	14	14	14
1995	Ave.	NA	NA	NA	NA	303	238	4.04	0.19	643	286	3.90	0.25
	SD	NA	NA	NA	NA	374	113	1.1	0.15	286	92	1.6	0.17
	No.	0	0	0	0	17	17	17	17	15	15	15	15

The standard deviation (SD) and number of cases are listed. The number of cases corresponds to the hours of sampling.

sulfate mass relationship is shown in Fig. 1. Solid squares represent the data for the PC air masses and open circles are for the C air masses. The regression equation for the best fit line is as given

$$\log CCN = (0.62 \pm 0.19)\log[SO_4^{2-}] + (2.2 \pm 0.17)\ cm^{-3} \quad (1)$$

with a correlation coefficient of 0.69. The sulfate mass ranged from ~8 to 28 μg m^{-3} and CCN concentrations ranged from 900 to 1800 cm^{-3} for the PC cases, whereas, the C cases had values of 1.5–7 μg m^{-3} for sulfate mass and between 160 and 700 cm^{-3} for CCN concentrations. The errors in CCN concentrations for these cases are on an average ~2% and are calculated as described in Section 2.2. Relatively high concentrations of CCN and sulfate were obtained for PC type air masses in conformity with previous findings of the enhancement of CCN concentrations due to anthropogenic emissions (Twomey et al., 1978; Hudson, 1991). Sulfate concentrations for the C cases differ by a factor of two from the PC cases though the CCN concentrations differ by more than a factor of four from the C to the PC cases. This suggests that either the CCN are generally smaller in the PC air masses or there are larger contribution from species other than sulfate in the PC cases compared with the C cases.

At high CCN concentrations, as more droplets compete for the same available water, the atmospheric supersaturation gets lowered due to the depletion of water vapor, thereby lowering the number of nuclei that would get activated. Therefore, this gives rise to an apparent lowered sensitivity of CCN concentrations at high sulfate values. Hence, the supersaturation, available liquid water in the cloud as well as variations in cloud base

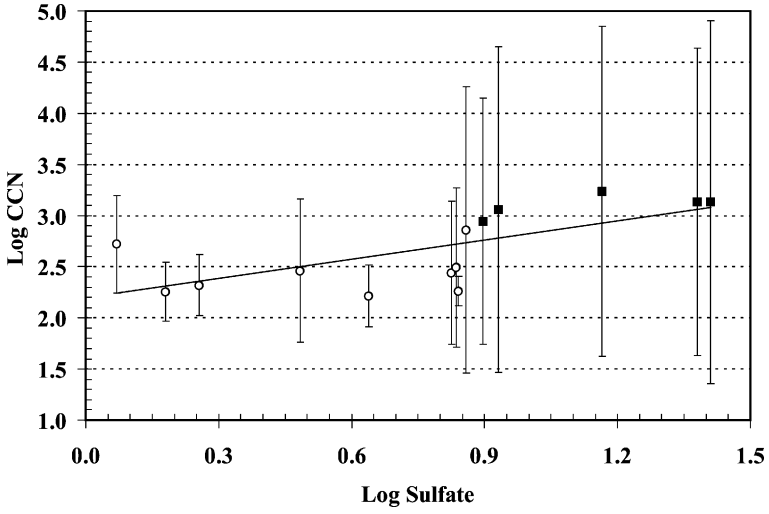

Fig. 1. Cloud condensation nuclei (CCN) concentrations (cm^{-3}) at 1% supersaturation as a function of sulfate mass concentration (μg m^{-3}). Solid squares are for the polluted continental cases and open circles are for continental cases.

updraft velocity (high updraft velocities would imply that a larger number of smaller droplets would be activated) give rise to the nonlinearity between CCN and sulfate concentration. In order to compare the sensitivity of CCN to sulfate at different locations, Saxena and Menon (1999) used a linear relationship between CCN-sulfate from the Mt. Mitchell data set and compared it to that of Hegg (1994) who had investigated the slopes of the CCN-sulfate mass relationships at four different locations — the NE Pacific, W Washington, NE Atlantic and Virginia Coast. For a linear relationship between CCN and sulfate, the slopes in Hegg (1994) ranged from 0.1 to 117 $m^3\ \mu g^{-1}\ cm^{-3}$ whereas, that in Saxena and Menon was 60 $m^3\ \mu g^{-1}\ cm^{-3}$. However, the regional variability of the slope and the decreasing values of the slopes with increasing sulfate concentrations imply that a non-linear relationship might be more realistic (Hegg, 1994).

Using measurements from previous years, a nonlinear relationship between CCN and N was obtained: given as $N = 183 \log (\mathrm{CCN}) - 334$ (Saxena and Menon, 1999). These are similar to results obtained by other investigators in the Northeast Atlantic (Gueltepe and Isaac, 1996). Similarly, the relationship between N and sulfate, obtained from prior results, suggested a higher sensitivity of N to sulfate for the Southeast as compared to results from Puerto Rico (Novakov et al., 1994) and the Northeast Atlantic (Leaitch et al., 1992), and are discussed in Menon and Saxena (1998). The non-linearities in CCN–sulfate, CCN–N and the N–sulfate relationships imply a reduced sensitivity of cloud optical depth and cloud albedo to anthropogenic aerosols that is investigated in the following sections.

4. Optical depth sensitivity

The relationship between cloud optical depth and cloud microphysical properties can be defined in terms of the number of droplets of a given radius that are contained in a cloud of depth, H, given as

$$\tau = 2\pi r_{\mathrm{rms}}^2 NH \tag{2}$$

where r_{rms} is the root mean square radius (Twomey, 1977). The optical depth can also be expressed as a function of LWC and R_{eff}, when LWC and R_{eff} are expressed as

$$\mathrm{LWC} = 4/3\pi r_{\mathrm{v}}^3 N\ \rho_{\mathrm{w}} \tag{3}$$

where r_{v} is the volume weighted moment of the drop size distribution, ρ_{w} is the density of water, and

$$R_{\mathrm{eff}} = r_{\mathrm{v}}^3 / r_{\mathrm{rms}}^2. \tag{4}$$

Ignoring differences between R_{eff}, r_{v} and r_{rms} as in Platinick and Twomey (1994), τ is then written as (Hansen and Travis, 1974)

$$\tau = (3\mathrm{LWC}^* H)/(2R_{\mathrm{eff}}\rho_{\mathrm{w}}). \tag{5}$$

Here, we assume both LWC and R_{eff} to be constant within the cloud since vertical variations in these quantities were not measured. Therefore, their values at cloud top will tend to be underestimated since LWC is known to increase with height within most clouds and R_{eff} is also expected to be the greatest at cloud top due to the increased LWC at cloud top.

The variations in τ arising from the variations in the cloud microphysical properties such as liquid water path (LWP, taken simply as the product of LWC and H), N and R_{eff} are analyzed by evaluating

$$\Delta\tau = \frac{\partial\tau}{\partial m}\Delta m \tag{6}$$

where m is one of the microphysical parameters and Δm is its change (Kogan et al., 1995). The sulfate content was categorized into two intervals ranging from $0 < \text{sulfate} < 300$ μmol l^{-1} and $300 < \text{sulfate} < 3000$ μmol l^{-1} to represent a less polluted and a polluted type air mass, respectively. By taking the derivative of Eqs. (2) and (5) and holding two of the parameters fixed, one can obtain the derivative of the optical depth for LWP, R_{eff} or N. The absolute value of the variation in τ to the changes in LWP, R_{eff} and N is shown in Fig. 2. The largest contribution arises from R_{eff} and LWP and is more than twice the contribution from N. Optical depth is more sensitive to changes in R_{eff} from polluted to less polluted type air masses. Since R_{eff} varies more with LWC and H than does N, variability in LWC and H in turn implies greater sensitivity of τ to R_{eff} than to N for differences in the cloud pollutant content.

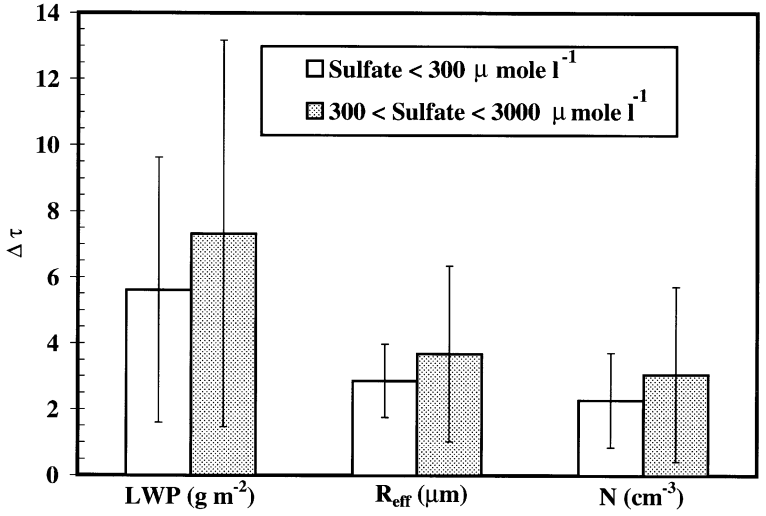

Fig. 2. Variation in cloud optical depth ($\Delta\tau$) caused by variations in the liquid water path (LWP) (g m^{-2}), cloud droplet number concentration (N) (cm^{-3}) and effective radii (R_{eff}) (μm) of cloud droplets. Data set is categorized as polluted ($300 < \text{sulfate content} < 3000$ μmol l^{-1}) and less polluted ($0 < \text{sulfate content} < 300$ μmol l^{-1}).

5. Influence of sulfates on cloud albedo

The sensitivity of cloud albedo to CCN or N, which is in turn related to the aerosol concentration and composition, is the essence of the albedo aspect of the Twomey effect. To determine changes in cloud albedo from polluted to less polluted clouds, cloud water sulfate is used as a surrogate for anthropogenic pollution: since prior measurements indicated high black carbon (BC) mass concentrations (a more suitable indicator of anthropogenic influence) were usually associated with high values of cloud water sulfate (Saxena and Menon, 1999). Deininger and Saxena (1997) and Menon et al. (2000) also found sulfates and nitrates to be most influential in cloud forming air masses from the PC sector, whereas for the M sector, sea salt particles were more abundant.

Cloud albedo was calculated from in situ observations as given in Lacis and Hansen (1974)

$$A = \tau/(\tau + 7.7). \tag{7}$$

The optical depth, τ, obtained by substituting Eq. (3) in Eq. (2) and ignoring differences in r_v and r_{rms} under the condition of constant LWC is expressed as

$$\tau = H\{4.5\pi N(\mathrm{LWC})^2\rho_w^{-2}\}^{1/3} \tag{8}$$

as in Platinick and Twomey (1994). Eqs. (2), (5) and (8) are all different parameterizations used to express optical depth as functions of N–R_{eff}, N–LWC and LWC–R_{eff}. These different parameterizations do not all result in the same optical depth since we ignore small differences in R_{eff}, r_v and r_{rms}. Differences also arise due to the lack of an agreement between LWC calculated from the ASRC collector and that estimated from the FSSP measurements (about $\sim$38%, based on the data described in Table 1). These differences could arise if the size distribution of droplets captured by the strings of the ASRC collector is different from that measured by the FSSP. Since the FSSP samples particles between 2 and 32 μm, presence of particles beyond this range could affect the estimated LWC. A more detailed discussion on the comparison of the LWC from the ASRC collector and the FSSP measurements are in Saxena et al. (1989) and DeFelice and Saxena (1990).

Cloud albedos calculated from in situ measurements were compared to the cloud albedos inferred from the AVHRR data, for cases that coincided with in situ observations. The AVHRR data retrieved from the NOAA-11, NOAA-12, and NOAA-14 satellites provide visible and near infrared radiances from which cloud albedo is inferred and has a spatial resolution of 1.1 km. The raw visible counts are scaled by the solar zenith angle and an anisotropic low (water) cloud reflectance factor is applied to determine the visible albedo. The same procedures and measurement criteria have been used to determine cloud albedo from satellite data as is given in Saxena et al. (1996). All convective type clouds were excluded from the analyses to avoid errors associated with inhomogeneous vertical stratification (Nakajima and King, 1990). Only warm orographic stratiform clouds formed in the vicinity if the Mt. Mitchell site were included. Out of the 14 cases discussed in Section 3, only three cases coincided with satellite measurements. Since they were all continental cases, five cases from the 1993–1994 field season were added in order to obtain differences in the albedo and sulfate content. A large number of cases for com-

parison of cloud albedos are difficult to obtain since a variety of conditions need to be fulfilled: e.g., non-precipitating cloud events, variable sulfate content in the cloud forming air mass, cloud thickness less than 300 m, coincidence of satellite passage with sampling period, etc. The conditions imposed for comparison as well as the five cases from the 1993–1994 field season are discussed in detail in Saxena et al. (1996).

The one-to-one relation between satellite inferred cloud albedo and that calculated from in situ measurements is indicated in Fig. 3. The correlation coefficient is about 0.90 for the eight cases and the 95% confidence interval for the correlation coefficient is between 0.58 and 0.98. Some uncertainty in determining cloud albedo from in situ measurements can be expected since vertical variations in R_{eff} and LWC within cloud depth were not determined and satellite inferred albedo is usually dependent on cloud top values. Also, the satellite data is obtained for a particular time period whereas in situ measurements are averaged for the whole hour, which might lead to some discrepancy, especially for cases where the cloud properties fluctuate during a particular hour. An agreement between the two data sets is however useful, since this would lead to confidence in using estimates of cloud albedo calculated from in situ measurements. If cloud albedo can be successfully determined using Eqs. (7) and (8), the relationships between cloud albedo and cloud chemistry/cloud microphysics can be investigated for a larger number of cases: due to the limited number of satellite inferred cloud albedo cases that are available.

Table 2 lists the cases and the associated variables such as cloud water sulfate, N, LWC, H and optical depth that were used for the cloud albedo comparison. Fig. 4 shows the cloud albedos from the AVHRR data (in filled squares) and all in-situ observations (in open circles) divided by the corresponding H, as a function of N. Since cloud albedo is sensitive to H, the cloud albedo was divided by the corresponding H. Due to the

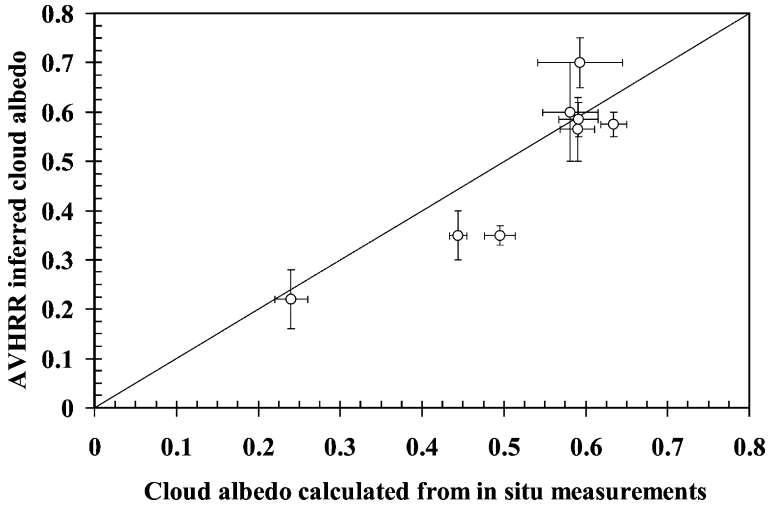

Fig. 3. Cloud albedo inferred from the Advanced Very High Resolution Radiometer (AVHRR) data versus that calculated from in situ measurements. The one-to-one correspondence line between them is given.

Table 2
Comparison of cloud albedo calculated from in situ measurements to that inferred from the Advanced Very High Resolution Radiometer (AVHRR) data, along with the coincident measurements of cloud water sulfate, cloud droplet number concentration (N), liquid water content (LWC), cloud thickness and cloud optical depth. Source of the cloud forming air mass is also given as marine (M), continental (C) or polluted continental (PC)

Dates	Source	$[SO_4^{2-}]$ (μmol l^{-1})	N (cm^{-3})	LWC (g m^{-3})	Cloud thickness (m)	Optical depth	In situ albedo (%)	AVHRR albedo $\lambda = 0.65$ μm (%)
14 Jun 1993	C	332	823±150	0.180	148±20	10.7±1.5	58.1±3.4	60.0±10.0
19 Jun 1993	M/C	81	218±160	0.190	238±51	11.4±2.4	59.8±5.2	70.0±5.0
19 Aug 1993	PC	555	613±100	0.150	105±5	6.1±0.3	44.2±1.1	35.0±5.0
21 Jul 1994	M	210	54±15	0.260	276±23	10.3±0.9	57.2±2.1	56.5±6.5
24 Jul 1994	C	52.5	231±91	0.070	101±10	2.5±0.3	24.8±2.0	22.0±6.0
9 Aug 1995	C	98.5	167±80	0.124	220±17	7.3±0.6	48.6±1.9	35.0±2.0
9 Aug 1995	C	191	167±56	0.166	268±28	10.8±1.2	58.3±2.4	58.5±3.5
10 Aug 1995	C	255.5	192±44	0.294	210±14	13.0±0.9	62.7±1.6	57.5±2.5

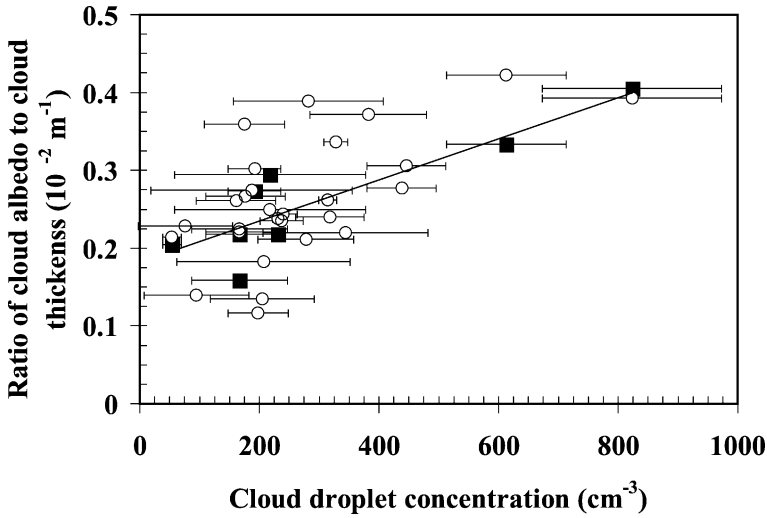

Fig. 4. Cloud albedo divided by the corresponding cloud thickness as a function of cloud droplet number concentration (N) (cm^{-3}). Filled squares are for cloud albedo inferred from the Advanced Very High Resolution Radiometer (AVHRR) data and open circles are for cloud albedo calculated from in situ observations. The linear trend is for the AVHRR inferred cloud albedo cases.

sensitivity of satellite inferred cloud albedo to the microphysical variables near cloud top, we chose cases where H were less than 300 m to minimize the effect of vertical variations of cloud properties on cloud albedo. Fig. 5 is similar to Fig. 4 but is for cloud albedo versus cloud water sulfate. Figs. 4 and 5 indicate that as N and cloud water sulfate increase, the cloud albedo thickness ratio also increases. However, the rate of increase in reflectance will decrease with increasing optical depth such that all but the most polluted clouds would have increased reflectance for an increase in the pollution content (Twomey, 1977). The slopes of the regressions indicated in Figs. 4 and 5 for the satellite inferred cloud albedo cases are 2.65×10^{-4} ($\pm5.9\times10^{-5}$) and 3.0×10^{-4} ($\pm1.54\times10^{-4}$), respectively. The correlation coefficient values are 0.88 and 0.63, respectively. For the cloud albedo calculated from in situ observations, there was a greater scatter in the data set. The wider distribution of points in Fig. 5 suggests a reduced sensitivity of cloud albedo to sulfate as compared to that between cloud albedo and N. This reduced sensitivity is to be expected since sulfates do not directly affect cloud albedo but through N, can affect cloud albedo. Using data from the four different locations Hegg (1994) calculated the change in cloud albedo for a fractional change in sulfate mass and N and found a reduced sensitivity of cloud albedo to sulfate variability as compared to CCN variability. Wigley (1991) had postulated that there could be an upper limit on the magnitude of forcing from sulfate.

Both Figs. 4 and 5 indicate that anthropogenic pollution over the continent play a role in changing the reflectivity of thin clouds. The reflectivity is also dependent on factors such as: variations in the updraft velocity that lead to variations in the number of nuclei activated, and the entrainment of dry air that could lead to evaporation or dilution of

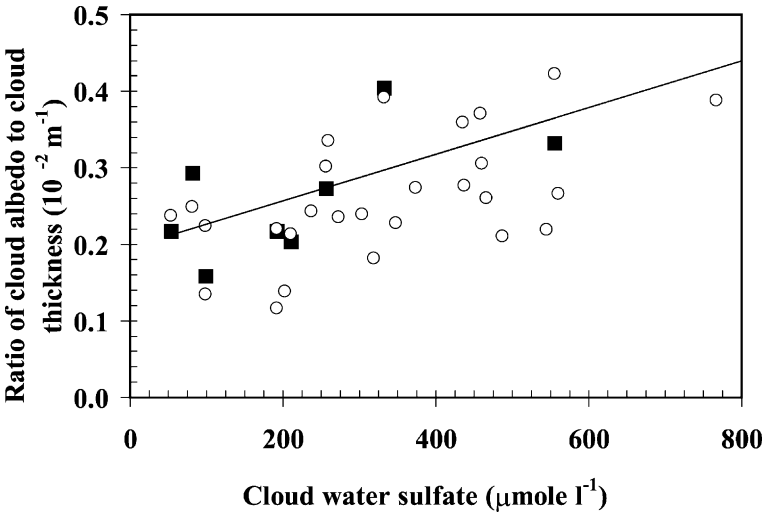

Fig. 5. Cloud albedo divided by the corresponding cloud thickness as a function of cloud water sulfate (μmol l^{-1}). Filled squares are for cloud albedo inferred from the Advanced Very High Resolution Radiometer (AVHRR) data and open circles are for cloud albedo calculated from in situ observations. The linear trend is for the AVHRR inferred cloud albedo cases.

droplets which can affect N and consequently the cloud albedo. The cloud albedo is also strongly related to changes in H and LWC as suggested by the scatter in the data set. Recent field studies in the North Atlantic by Brenguier et al. (2000) also suggest that the cloud radiative properties are quite sensitive to cloud thickness and LWP. Since both R_{eff} and LWC vary with height within cloud depth and large variations in LWC can occur even in clouds 300 m thick, the location of the sampling site with respect to cloud base needs to be ascertained, as the fixed elevation of the sampling site implies that clouds could be sampled at various vertical levels. This could lead to additional uncertainty in accurately determining the sensitivity of cloud albedo to sulfate and N. Orographic influences could also lead to additional complexity in determining the variability in N, R_{eff} and LWC with H.

In terms of the indirect forcing effect of sulfates, for the first time we have been able to demonstrate the increase in cloud albedo with sulfate and N for the southeastern US using surface-based observations and satellite retrievals. Similar observational evidence of changes in cloud radiances and microphysics in marine and polluted air masses for stratocumulus clouds in the Northeast Atlantic have recently been reported by Brenguier et al. (2000).

6. Conclusions

The air masses that traversed from the polluted sectors in the Ohio River Valley region to the southeastern US were found to have higher sulfate levels and higher CCN

concentrations. The best-fit line for the CCN-sulfate regression equation was for a non-linear trend. The above result is for cases where we make the assumption that the entire sulfate in the air mass gets scavenged in cloud water. This gives us a first order estimate of the modification in CCN concentration that result from sulfates. Average values of N and sulfate were much higher for the polluted type air masses than for the continental and marine air masses.

Despite a larger difference in the average values of N as compared to that for R_{eff} between polluted and less polluted air masses, the optical depth was found to be more sensitive to variations in R_{eff} from polluted to less polluted air masses due to the variability in the LWP. The cloud albedo calculated from in situ measurements for eight cases from a 3-year period (1993–1995) was verified with that inferred from the AVHRR data. This is a significant result of our closure experiment. Cloud water sulfate was used as a surrogate for anthropogenic pollution. The cloud albedo divided by the corresponding cloud thickness was found to increase with an increase in the cloud water sulfate and N. The scatter in the data suggests that cloud albedo is sensitive to H and LWC. Non-linear increases in satellite inferred cloud albedo with LWP, shown in Fig. 6, suggest the importance of determining the contribution of cloud dynamic feedbacks on the indirect effect as pointed out by Han et al. (1998). Such effects have recently started getting more attention.

The transport of anthropogenic emissions over the continent influenced the micro-physical and optical properties of cloud forming air masses that arrived at our remote mountaintop site in the southeastern US. Measurements that relate the production and the transport of aerosols to cloud microphysical and optical properties should be made at a number of different locations due to the regional radiative forcing effect of aerosols.

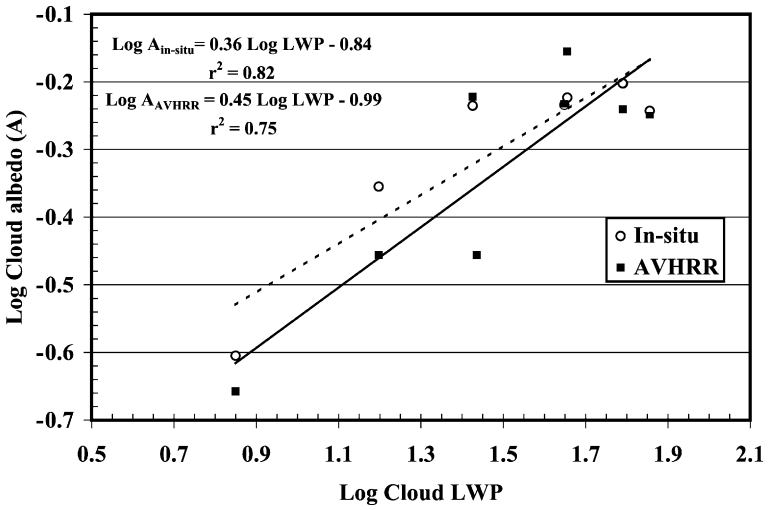

Fig. 6. Cloud albedo inferred from the Advanced Very High Resolution Radiometer (AVHRR) data versus cloud liquid water path (LWP) (g m^{-2}). The trend line for the AVHRR data is the solid line and the dashed line is for in-situ measurements.

Appropriate parameterizations can then be employed by climate models to fully assess and verify the role of anthropogenic aerosols in modifying global climate.

Acknowledgements

This research was supported through the Southeast Regional Center for the National Institute for Global Environmental Change, Tuscaloosa, AL, by the US Department of Energy under co-operative agreement DE-FCO3-90ER61010 (50%) and by the US Environmental Protection Agency through STAR Grant R-825248 (50%). We thank the Cloud Physics Group for help in the fieldwork and Dr. W.P. Robarge from the NCSU Soil Sciences laboratory for the chemical analyses. Encouragement received from Prof. R. Griffin and Mr. W. Herz is greatly appreciated. We appreciate the discussions with Prof. R.R. Braham. The comments of the two anonymous reviewers are greatly appreciated.

References

Baumgardner, D., 1983. An analysis and comparison of five water droplet measuring instruments. J. Clim. Appl. Meteorol. 22, 891–910.

Boers, R., Ayers, G.P., Gras, J.L., 1994. Coherence between seasonal variation in satellite-derived cloud optical depth and boundary layer CCN concentrations at a mid-latitude southern hemisphere station. Tellus 46B, 123–131.

Borys, R.D., Lowenthal, D.H., Wetzel, M.A., Herrera, F., Gonzalez, A., Harris, J., 1998. Chemical and microphysical properties of marine stratiform cloud in the North Atlantic. J. Geophys. Res. 103, 22073–22085.

Boucher, O., Lohmann, U., 1995. The sulfate-CCN-cloud albedo effect: a sensitivity study with two general circulation models. Tellus 47B, 281–300.

Brenguier, J.L., Pawlowska, H., Schuller, L., Preusker, R., Fischer, J., Fouquart, Y., 2000. Radiative properties of boundary layer clouds: droplet effective radius versus number concentration. J. Atmos. Sci. 57, 803–821.

Charlson, R.J., Lovelock, J.E., Andreae, M.O., Warren, S.G., 1987. Oceanic phytoplankton, atmospheric sulphur, cloud albedo and climate. Nature 326, 655–661.

Charlson, R.J., Langner, J., Rodhe, H., Leovy, C.B., Warren, S.G., 1991. Perturbation of the northern hemisphere radiative balance by backscattering from anthropogenic sulfate aerosols. Tellus 43AB, 152–163.

Chuang, C.C., Penner, J.E., Taylor, K.E., Grossman, A.S., Walton, J.J., 1997. An assessment of the radiative effects of anthropogenic sulfate. J. Geophys. Res. 102, 3761–3778.

DeFelice, T.P., Saxena, V.K., 1990. Mechanisms for the operation of three cloud water collectors: comparison of mountain-top results. Atmos. Res. 25, 277–292.

DeFelice, T.P., Saxena, V.K., 1994. On the variation of cloud condensation nuclei in association with cloud systems at a mountain-top location. Atmos. Res. 31, 13–39.

Deininger, C.K., Saxena, V.K., 1997. A validation of back trajectories of air masses by principal component analysis of ion concentrations in cloud water. Atmos. Environ. 30, 295–300.

Dettinger, M.D., Ghil, M., Keppenne, C.L., 1995. Interannual and interdecadal variability in United States surface-air temperatures, 1910–87. Clim. Change 31, 35–66.

Draxler, R.R., 1987. Sensitivity of a trajectory model to the spatial and temporal resolution of the meteorological data during CAPTEX. J. Clim. Appl. Meteorol. 26, 1577–1588.

Draxler, R.R., Stunder, B.J.B., 1988. Modeling the CAPTEX vertical tracer concentration profiles. J. Appl. Meteorol. 27, 617–625.

Environmental Protection Agency (EPA), 1993. Emission Summaries of Air Quality Planning and Standards, Research Triangle Park, NC. Regional Emission Inventories (1987–1991), vol. II.

Fukuta, N., Saxena, V.K., 1979a. A horizontal thermal gradient cloud condensation nucleus spectrometer. J. Appl. Meteorol. 18, 1352–1362.

Fukuta, N., Saxena, V.K., 1979b. The principle of a new horizontal thermal gradient cloud condensation nucleus spectrometer. Atmos. Res. 13, 169–188.

Garrett, T.J., Hobbs, P.V., 1995. Long-range transport of continental aerosols over the Atlantic Ocean and their effects on cloud structures. J. Atmos. Sci. 52, 2977–2984.

Ghan, S.J., Easter, R., Hudson, J., Breon, F.-M., 2001. Evaluation of aerosol indirect forcing in MIRAGE. J. Geophys. Res. 106, 5317–5334.

Gueltepe, I., Isaac, G.A., 1996. The relationship between cloud droplet and aerosol number concentrations for climate models. Intl. J. Climatol. 16, 941–946.

Han, Q., Rossow, W.B., Chou, J., Welch, R.M., 1998. Global survey of cloud albedo and liquid water path with droplet size using ISCCP. J. Clim. 11, 1516–1528.

Hansen, J.E., Travis, L.D., 1974. Light scattering in planetary atmospheres. Space Sci. Rev. 16, 527–610.

Hegg, D.A., 1994. Cloud condensation nucleus-sulfate mass relationship and cloud albedo. J. Geophys. Res. 99, 25903–25907.

Hegg, D.A., Hobbs, P.V., 1983. Preliminary measurements of the scavenging of sulfate and nitrate by clouds. In: Pruppacher, H.R., Semonin, R.G., Slinn, W.G.N. (Eds.), Precipitation Scavenging, Dry Deposition and Resuspension, vol 1. Elsevier, New York, pp. 79–89.

Hegg, D.A., Livingston, J., Hobbs, P.V., Novakov, T., Russell, P., 1997. Chemical apportionment of aerosol column optical depth off the mid-Atlantic coast of the United States. J. Geophys. Res. 102, 25293–25303.

Hudson, J.G., 1991. Observations of anthropogenic cloud condensation nuclei. Atmos. Environ. 25A, 2449–2455.

Hudson, J.G., Li, H., 1995. Microphysical contrasts in Atlantic stratus. J. Atmos. Sci. 52, 3031–3040.

Jones, A., Robert, D.L., Slingo, A., 1994. A climate model study of indirect radiative forcing by anthropogenic sulfate aerosols. Nature 370, 450–453.

Kadlecek, J., McLaren, S., Camarota, N., Mohnen, V., Wilson, J., 1983. Cloud water chemistry at Whiteface Mountain. In: Pruppacher, H.R., Semonin, R.G., Slinn, W.G.N (Eds.), Precipitation, Scavenging, Dry Deposition, and Resuspension, vol. 1. Elsevier, New York, pp. 103–114.

Knollenberg, R.G., 1981. Techniques for probing cloud microstructure. In: Hobbs, P.V., Deepak, A. (Eds.), Clouds, Their Formation, Optical Properties, and Effects, Academic Press, San Diego, CA, pp. 15–91.

Kogan, Z.N., Kogan, Y.L., Lilly, D.K., 1995. The effects of stratocumulus cloud layer microphysics on its optical depth. Preprint Vol. Conf. on Cloud Physics, AMS, Dallas, TX, pp. 74–79.

Kondratyev, K.Ya., 1999. Climatic Effects of Aerosols and Clouds Springer-Praxis, New York, 264 pp.

Lacis, A.A., Hansen, J.E., 1974. A parameterization of the absorption of solar radiation in the earth's atmosphere. J. Atmos. Sci. 31, 118–133.

Leaitch, W.R., Strapp, J.W., Isaac, G.A., 1986. Cloud nucleation and cloud scavenging of aerosol sulphate in polluted atmospheres. Tellus 38B, 328–344.

Leaitch, W.R., Isaac, G.A., Strapp, J.W., Banic, C.M., Wiebe, H.A., 1992. The relationship between cloud droplet number concentration and anthropogenic pollution: observations and climatic implications. J. Geophys. Res. 97, 2463–2474.

Leaitch, W.R., Banic, C.M., Isaac, G.A., Couture, M.D., Liu, P.S.K., Gueltepe, I., Li, S.-M., Kleinman, L., Daum, P.H., MacPherson, J.I., 1996. Physical and chemical observations in marine starus during the 1993 North Atlantic Regional Experiment: factors controlling cloud droplet number concentrations. J. Geophys. Res. 101, 29123–29135.

Lohmann, U., Feichter, J., 1997. Impact of sulfate aerosols on albedo and lifetime of clouds: a sensitivity study with the ECHAM4 GCM. J. Geophys. Res. 102, 13685–13700.

Lohmann, U., Feitcher, J., Chuang, C.C., Penner, J.E., 1999. Prediction of the number of cloud droplets in the ECHAM GCM. J. Geophys. Res. 104, 9169–9198.

McLaren, S., Kadlecek, S.J., Kadlecek, A., Spencer, J., Conway, C., 1985. Field intercomparison of cloud water collectors at Whiteface Mountain. Report from the Whiteface Mountain Field Station, Wilmington, NY 12997. Atmospheric Science Research Center, Albany, NY, 66 pp.

Menon, S., Saxena, V.K., 1998. Role of sulfates in regional cloud–climate interactions. Atmos. Res. 47–48, 299–315.

Menon, S., Saxena, V.K., Logie, B.D., 2000. Chemical heterogeneity across cloud droplet size spectra in continental and marine air masses. J. Appl. Meteorol. 39, 887–903.

Menon, S., Del Genio, A.D., Koch, D., Tselioudis, G., 2001. GCM simulations of the aerosol indirect effect: Sensitivity to cloud parameterization and aerosol burden. J. Atmos. Sci., in press.

Nakajima, T., King, M.D., 1990. Determination of the optical thickness and effective particle radius of clouds from reflected solar radiation measurements: Part I. Theory. J. Atmos. Sci. 47, 1878–1893.

Novakov, T., Penner, J.E., 1993. Large contribution of organic aerosols to cloud-condensation–nuclei concentrations. Nature 365, 823–826.

Novakov, T., Rivera-Carpio, C., Penner, J.E., Rogers, C.F., 1994. The effect of anthropogenic sulfate aerosols on marine cloud droplet concentrations. Tellus 46B, 132–141.

Novakov, T., Hegg, D.A., Hobbs, P.V., 1997. Airborne measurements of carbonaceous aerosols on the East Coast of the United States. J. Geophys. Res. 102, 30023–30030.

Platinick, S., Twomey, S., 1994. Determining the susceptibility of cloud albedo to changes in droplet concentration with the Advanced Very High Resolution Radiometer. J. Appl. Meteorol. 33, 334–347.

Rivera-Carpio, C.A., Corrigan, C.E., Novakov, T., Penner, J.E., Rogers, C.F., Chow, J.C., 1996. Derivation of contributions of sulfates and carbonaceous aerosols to cloud condensation nuclei from mass size measurements. J. Geophys. Res. 101, 19483–19493.

Rotstayn, L.D., 1999. Indirect forcing by anthropogenic aerosols: a global climate model calculation of the effective radius and cloud-lifetime effects. J. Geophys. Res. 104, 9369–9380.

Saxena, V.K., Lin, N.-H., 1990. Cloud chemistry measurements and estimates of acidic deposition on an above cloudbase coniferous forest. Atmos. Environ. 24A, 329–352.

Saxena, V.K., Menon, S., 1999. Sulfate-induce cooling in the southeastern U.S.: an observational assessment. Geophys. Res. Lett. 26, 2489–2492.

Saxena, V.K., Stogner, R.E., Hendler, A.H., DeFelice, T.P., Yeh, R.J.-Y., 1989. Monitoring the chemical climate of the Mt. Mitchell State Park for evaluation of its impact on forest decline. Tellus 41B, 92–109.

Saxena, V.K., Durkee, P.A., Menon, S., Anderson, J., Burns, K.L., Nielsen, K.E., 1996. Physico-chemical measurements to investigate regional cloud–climate feedback mechanisms. Atmos. Environ. 30, 1573–1579.

Saxena, V.K., Yu, S.-C., Anderson, J., 1997. Impact of stratospheric volcanic aerosols on climate: evidence for aerosol shortwave and longwave forcing in the southeastern U.S. Atmos. Environ. 31, 4211–4221.

Schwartz, S.E., Slingo, A., 1996. Enhanced shortwave cloud forcing due to anthropogenic aerosols. In: Crutzen, P.J., Ramanthan, V. (Eds.), NATO AS1 Series. Springer-Verlag, Berlin, pp. 191–236.

Twomey, S., 1977. Influence of pollution on the shortwave albedo of clouds. J. Atmos. Sci. 34, 1149–1152.

Twomey, S., Davidson, A.K., Seton, K.J., 1978. Results of five years' observations of cloud nucleus concentration at Robertson, New South Wales. J. Geophys. Res. 35, 650–656.

Ulman, J.C., Saxena, V.K., 1997. Impact of air mass histories on the chemical climate of Mount Mitchell, North Carolina. J. Geophys. Res. 102, 25451–25465.

Wigley, T.M.L., 1991. Could reducing fossil fuel emissions cause global warming? Nature 349, 503–506.